ACS APPLIED ENERGY MATERIALS

www.acsaem.org

Article

CMC Staining Method for the Visualization of the Binder Distribution in Water-Based Electrodes with EDS

Noah Keim,* Andreas Weber, Marcus Müller, David Burger, Werner Bauer, Philip Scharfer, Wilhelm Schabel, and Helmut Ehrenberg

Cite This: https://doi.org/10.1021/acsaem.5c00048

Read Online

ACCESS | Metrics & More | Article Recommendations | Supporting Information

ABSTRACT: The selective staining of cellulose materials is crucial for the accurate investigation of the binder distribution in electrodes of lithium-ion batteries. This paper investigates how (heptadecafluorodecyl)-trimethoxysilane selectively reveals the binder distribution via EDS. Selectivity was granted by investigating individual electrode components: graphite, carbon black (CB), styrene−butadiene rubber (SBR), and sodium carboxymethyl cellulose (NaCMC). Each component was treated with the staining agent, stored at 60 °C for 16 h, washed with ethanol, and analyzed via energy dispersive spectroscopy (EDS). Only NaCMC shows a significant increase in fluorine concentration, proving selective staining. The study further explores the reaction mechanism by varying the degree of substitution (DS) of NaCMC, showing a correlation between carboxyl moieties and fluorine concentration and identifies 16 h of heated storage as a viable staining condition. Finally, the method's applicability was demonstrated by comparing binder distribution in electrodes dried at different rates, revealing the NaCMC binder distribution via EDS.

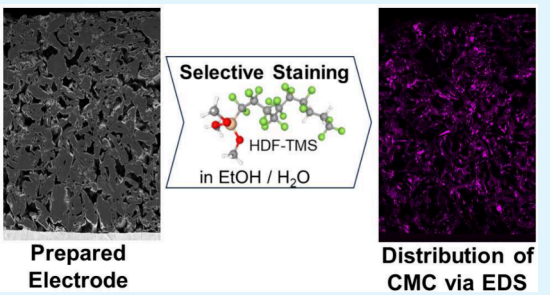

KEYWORDS: *NaCMC, Electrode processing, Binder migration, Selective staining method, EDS*

INTRODUCTION

Polyvinylidene fluoride (PVDF) still remains the industry's standard binder for producing homogeneous and stable slurries in lithium-ion battery cathode production. It is known for its excellent electrochemical stability, being an efficient dispersion agent for conductive additives within the slurry, and its favorable electrolyte wettability.[1−5] But PVDF has well-known drawbacks when used as an electrode binder, including its PFAS classification and the requirement for *N*-methyl-2-pyrrolidone (NMP) as a solvent, which poses environmental and health risks.[3,5−8] Despite these issues, PVDF offers a significant advantage for battery research and development: its fluorine content makes it easily traceable by spectroscopic methods, allowing for a thorough understanding of how processing conditions and polymer parameters affect binder distribution.[9] Especially for strong binder migration when increasing the drying rate or electrode thickness, direct microstructure−property relationships between cell performance and binder distribution could be made observable.[10]

Water-based processing for graphite anodes has already been established in industrial-scale manufacturing for many years, with various publications confirming its superior performance.[5,11−13] The distributions of styrene−butadiene rubber (SBR) and sodium carboxymethyl cellulose (NaCMC) both have a significant impact on electrode properties and cell performance, and therefore understanding the distribution would help further improve both. As publications have shown, the ion used for creating the CMC salt has an influence on the cell performance; hence, it is necessary to annotate the used cation in the CMC.[13−16] While the selective staining of SBR was achieved by Lee et al.,[17] understanding the distribution of cellulose-based cobinders like NaCMC within these electrodes remains difficult. The amount of sodium atoms in the final electrode is too small to be readily detected in electrode cross sections by spectroscopic means. Therefore, the main challenge is the lack of an effective staining method, as these polymers lack easily traceable heteroatoms, limiting the use of conventional techniques like energy-dispersive X-ray spectroscopy (EDS), which is commonly used for PVDF.[9] The objective of this paper is to address this gap, by showcasing a staining agent specifically for cellulose-based cobinders. Other preliminary investigations trying to properly stain CMC failed due to various challenges, like dissolving the CMC, drastic side reactions with other components of the electrode, or the concentration of the staining agent being too low to properly depict the CMC properly. The agent overcomes the limitations of those other methods by ensuring an accurate binder

Received: January 8, 2025
Revised: March 7, 2025
Accepted: March 10, 2025

distribution analysis without altering the binder distribution itself. It reacts specifically with the cellulose cobinder, offering a reliable solution for detailed analysis of binder distribution in water-based electrode systems.

EXPERIMENTAL SECTION

Materials. The main focus of this investigation is the staining of varying cellulose-based binders used in graphite electrodes. If not stated otherwise, the following composition was used for electrodes regarding the chapter selectivity of the staining agent: 96 wt % of graphite (natural, MechanoCap 1P1, H.C. CARBON, Germany), 1.5 wt % of carbon black (CB, C-NERGY Super C65, Imerys Graphite & Carbon, Switzerland), 1.25 wt % of SBR binder (TRD 2001, JSR Micro, Belgium), and 1.25 wt % of NaCMC (IFF Specialty Products, Germany). The current collector of the electrode was copper (PHC, SE-Cu58). The areal capacity for the anodes was set at 2.1 ± 0.1 mAh cm^{-2}. The electrodes were prepared by mixing using a dissolver (Dispermat CA60, VMA Getzmann, Germany) with a 50 mm toothed disk in a batch container (volume 250 mL). The container was placed in a water-cooled casing. In a prepared 2 wt % solution of NaCMC in deionized water, a powder mixture of graphite and CB was added continuously while stirring at 500 rpm for 15 min. After the addition of the active material, the slurry was dissolved for 45 min at 2000 rpm. To add the shear sensitive SBR, the stirring speed was reduced to 300 rpm and combined with degassing the slurry (approximately 200 hPa). The water content was adjusted to create a solid content of 56 wt %. Electrodes were produced via roll-to-roll coating (KTFS, Mathis AG, Switzerland) with a doctor blade and a wet-film thickness of 75 μm. The two separate drying chambers had temperatures of 25 and 30 °C, while the coating was limited to a web speed of 0.2 m min^{-1}.

Electrodes regarding the chapter application had the composition of 93 wt % of graphite (SMGA, Hitachi Chemical Co. Ltd., Japan), 1.4 wt % of carbon black (CB, C-NERGY Super C65, Imerys Graphite & Carbon, Switzerland), 3.73 wt % of SBR binder (Zeon Europe GmbH, Japan), and 1.87 wt % of cellulose based binder. Again, the current collector was made of copper (Civen Metal Material Co. Ltd., China). The areal capacity for the anodes was set at 4.0 ± 0.1 mAh cm^{-2}. Here, the slurry for the electrode was mixed in a dissolver (Dispermat SN-10, VMA Getzmann GmbH Verfahrenstechnik, Germany), and the container was cooled with water during the process. First, the CB was dispersed in a 2 wt % CMC solution at 1500 rpm for 30 min. Afterward, the graphite was added in three separate steps with a short mixing sequence of 1 min at 400 rpm. Further water was added for the final solid content to be reached at 43 wt %. A second dispersion step followed (30 min at 1500 rpm). Finally, the SBR dispersion was added, and the slurry was mixed for 10 min at 500 rpm and degassed. The slurries were coated and dried in a discontinuous process. The slurry was doctor bladed (ZUA 2000.60, Zehntner GmbH, Switzerland). The coatings were dried differently to create electrodes with a low drying rate (0.75 g m^{-2} s^{-1}) and a high drying rate (6 g m^{-2} s^{-1}). Further details regarding the manufacturing are described by Burger et al.[18] All electrodes were calendered to equal a porosity of 50%.

Decorating of NaCMC with (Heptadecafluorodecyl) Trimethoxysilane. To detect cellulose based binders in dried electrodes, they were selectively decorated with (heptadecafluorodecyl)-trimethoxysilane (HDF-TMS, ABCR, Germany). HDF-TMS was diluted with ethanol (absolute, VWR) to create a 0.2% (v/v) solution. Before using it as staining agent the same volume of deionized water, in regard to HDF-TMS, was added to the solution and premixed for 15 min to allow the methoxysilane to hydrolyze; see Figure 1.

For a 1 cm^2 electrode, this meant using 0.98 mL of ethanol, with 20 μL of HDF-TMS, resulting in 20 μL of water being used for hydrolysis. The dried anode was submerged in the solution and stored at elevated temperature of 60 °C for 16 h to allow for the condensation reaction of the silane with the cellulose binder to take place. Afterward, the electrode was submerged in ethanol for a minimum of 2 h and washed multiple times with ethanol to extract

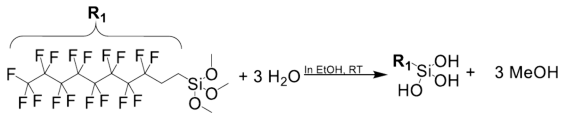

Figure 1. Hydrolysis of the HDF-TMS with water, leading to activation of the HDF-TMS.

excess HDF-TMS and dried in the atmosphere for at least 4 h; see Figure 2.

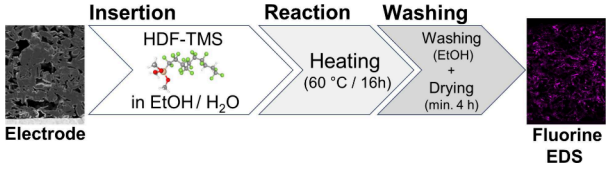

Figure 2. Schematic representation of the staining process used for graphite anodes with NaCMC binder.

For preliminary samples of pure electrode components, 500 mg each was used and stained in 1.0 mL of prepared HDF-TMS solution. CB and graphite were pressed into pellets with diameters of 12 mm. The SBR suspension was dried, and 500 mg of the resulting latex film was used, while a film of pure NaCMC was prepared. The pure film was prepared out of a 2 wt % aqueous solution.

SEM and EDS. Scanning electron microscopy (SEM) was performed operating at an acceleration voltage of 2 kV by using a Gemini system (Carl Zeiss, Germany). For elemental analysis, energy-dispersive spectroscopy (EDS) was conducted with an Ultim Extreme Detector (Oxford Instruments, United Kingdom) at a 4 kV acceleration voltage. The cross section of stained electrode samples was prepared by broad ion beam milling with a TIC3X instrument (Leica Microsystems, Germany).

RESULTS AND DISCUSSION

Selectivity of the Staining Agent. To properly represent the binder distribution, the staining agent must selectively stain the cellulose binder and not any other component of the electrode. To investigate possible side reactions, every single electrode component (graphite, CB, SBR, and NaCMC) was analyzed individually. Every material was prepared as a separate sample, submerged in the staining agent, stored for 16 h at 60 °C, washed with ethanol, and dried. The sample surface then was analyzed via EDS, measuring the elemental composition; see Table 1.

Table 1. EDS Composition (atom %) of the Surface Area of Electrode Component Exposure to the Staining Agent

Sample	Carbon	Oxygen	Fluorine	Silicon	Sodium
Graphite	99.2	0.3	0.4	0.04	
CB	99.4	0.5	0.07		
SBR	88.1	8.2	0.2		1.9
NaCMC	25.3	4.7	44.4	2.4	0.06

Every component, other than the NaCMC, shows very low amounts of residual fluorine, with none exceeding 0.4 atom % of fluorine. This is especially true for the conductive additive CB, which we expected to have the highest amount of residual fluorine due to its high surface area. Unexpectedly, CB even shows the lowest amount of fluorine with only 0.07 atom % of fluorine, coming close to the lower detection limit of the EDS. While SBR also shows a very low amount of fluorine concentration on the surface, a very high oxygen, sulfur, and

https://doi.org/10.1021/acsaem.5c00048
ACS Appl. Energy Mater. XXXX, XXX, XXX−XXX

sodium content is measured (see Figure S1). Commonly, surfactants like sodium dodecyl sulfate are used to stabilize the SBR suspension, to which we attribute the results.[19] Additionally, this allows us to exclude the surfactant as a potential side reactant, as there is no increase in fluorine detectable.

Only NaCMC shows a significant increase in fluorine concentration with more than 44 atom %. This proves that the staining agent mainly reacts with the NaCMC, while the other electrode components remain largely unaffected. While studying the behavior of the individual anode materials serves as a proof of concept, the staining method has to be verified in a real application. For that reason, it is crucial to selectively mark the cellulosic binders in porous electrodes and remove excess staining agents after the reaction. To evaluate the likeliness of residual agent (that has not reacted with the binder) accumulating in the pores between active materials, an electrode was submerged into the staining agent for 16 h, without any heating to slow the condensation reaction. After the sample was washed with ethanol, the cross section of the electrode was prepared. EDS reveals that there is no significant accumulation of staining agent in between or inside of the active material; see Figure 3. To compare visibility for varying EDS signals, an SEM micrograph with the corresponding EDS mapping results are shown beside each other.

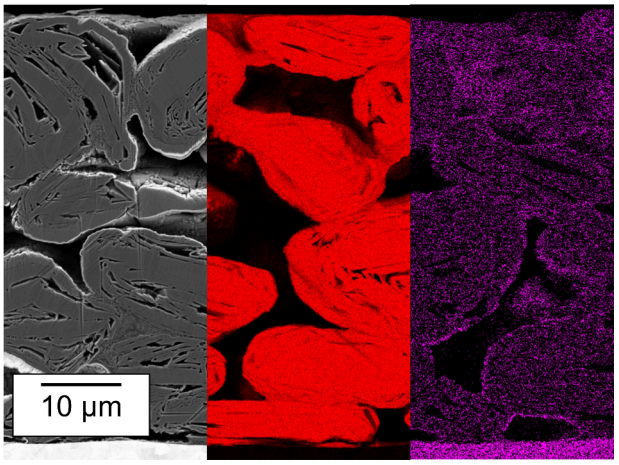

Figure 3. (left) SEM micrograph of electrode cross section stored in staining agent at ambient conditions for 16 h. (middle) Partially superimposed EDS mapping results of the electrode for carbon (red) (right) Corresponding EDS mapping results of the electrode for fluorine (magenta).

The measured amount of fluorine is at a maximum of 0.11 atom % throughout the whole cross section. The EDS measurement in the middle of Figure 3 displays the carbon distribution, while for the fluorine measurement artifacts are shown instead of a real distribution of fluorine across the electrode. Even when focusing on an agglomerate of CB (see Figure S2), the concentration does not exceed 0.1 atom % of fluorine, further underlining that HDF-TMS is not adsorbing to the carbon surface of the conductive additive. By this, it is shown that washing with ethanol effectively allows for the extraction of excess agent, leaving minimal residue close to the lower detection limit. HDF-TMS has to react with the cellulose binder to allow for detection and otherwise is going to be washed away by ethanol. Having established the selectivity of the process, we next examined the possible mechanisms. By an increase in the degree of substitution (DS) of the NaCMC in the anodes, the absolute number of carboxyl moieties increases. We therefore varied the NaCMC in the electrodes to investigate whether the hydroxy or carboxyl moieties are key for the reaction with HDF-TMS. Gadhave et al.[20] proposed that for pure cellulose the silane is reacting with the hydroxy moieties, but our result strongly suggests that this is not transferable to NaCMC. The lowest DS of 0.4 also shows the lowest signal for fluorine with only 0.9 ± 0.1 atom %, while it increases for DS 0.7 to 1.5 ± 0.1 atom % and is highest for DS 0.9 with 3.0 ± 0.1 atom % (for detailed EDS results, see Figure S3). The increase of fluorine concentration is therefore attributed to the increase in carboxyl moieties, suggesting the reaction mechanism given in Figure 4.

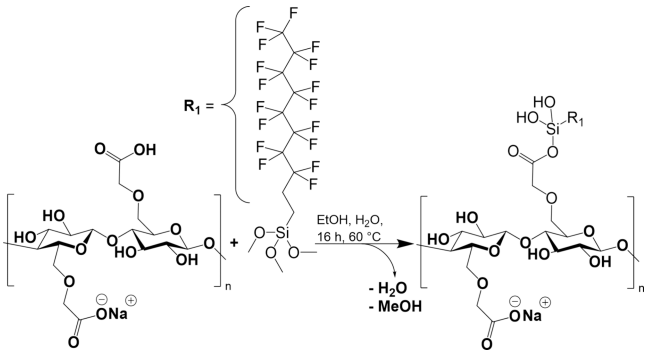

Figure 4. Possible reaction mechanism of HDF-TMS with CMC. MeOH and EtOH are abbreviations for methanol and ethanol, respectively.

By varying the storage times in the staining agent at elevated temperature, it was possible to identify the conditions for a reliable staining of the NaCMC; see Figure 5.

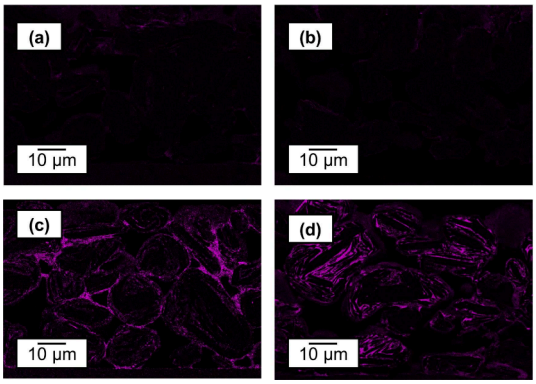

Figure 5. Results for varying storage times in the staining agent. Fluorine EDS mapping after (a) 4 h, (b) 8 h, (c) 16 h, and (d) 60 h. For details regarding EDS, see Figure S4.

By an increase in the storage time, the fluorine concentration in the cross section increases continuously. Results from this investigation demonstrate that the staining process is time-dependent, with sufficient results being achieved after 16 h of heated storage. This duration provides good staining visibility, as shown by the individual samples. Too short exposure times (less pronounced staining) could lead to an inaccurate interpretation of the binder distribution. This is in line with the fluorine concentration, which is lowest for the 4 h storing time with 0.46 ± 0.06 atom % and increases further to 1.1 ± 0.1 atom % fluorine for 8 h and reaches 1.5 ± 0.1 atom % after

https://doi.org/10.1021/acsaem.5c00048
ACS Appl. Energy Mater. XXXX, XXX, XXX−XXX

16 h. A longer duration of staining leads to a further increase in fluorine content, as 60 h shows 4.4 ± 0.1 atom %. The further increase in fluorine is attributed to the further reaction of the silane as a self-condensation reaction.[21] The self-condensation leads to excess silane to react with itself rather than with further NaCMC. When the fluorine content is increased, the representation of the NaCMC does not become more distinct in the EDS mapping.

Application in Electrodes. This staining method is particularly valuable for gaining deeper insight into how different processing and polymer parameters affect the binder distribution within the electrode. Therefore, we want to showcase one application for the staining method, by investigating the binder distribution for a lower drying rate (LDR) and a higher drying rate (HDR); see Figure 6.

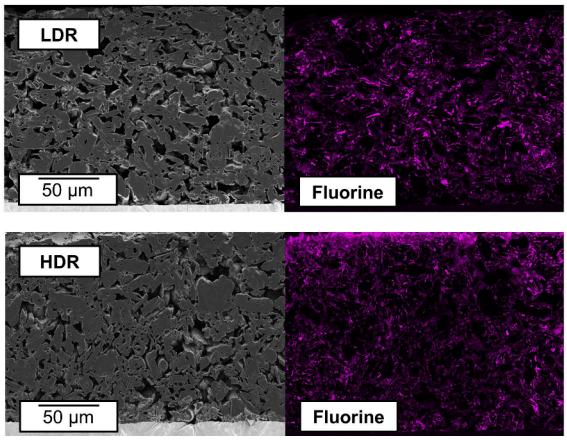

Figure 6. SEM micrographs for lower drying rate (slow drying) and higher drying rate (fast drying) electrodes with corresponding EDS mapping of fluorine (magenta) on the right.

The measurement via EDS reveals that the overall amount of fluorine (average over entire cross section) is the same for both slow- and fast-dried electrodes, with levels around 4.7 ± 0.3 atom %. This is to be expected, as the electrodes have the same composition. The same amount of fluorine suggests that the reaction takes place regardless of the local concentration of NaCMC and works as a tracer for NaCMC. When the electrode cross section is examined more closely by dividing it into distinct areas, namely the lower, middle, and upper thirds, a noticeable variation in the distribution of NaCMC becomes apparent; see Table 2.[9] It has to be noted that the redeposition of the copper during ion milling covers parts of the electrode and leads to a higher concentration of copper in the lower third, which could impact the elemental composition of the EDS.

Table 2. Fluorine Concentration (in atom % F) for Different Thirds of the Electrode, Determined via EDS

Section	Low Drying Rate	High Drying Rate
Upper	3.9 ± 0.8	6.1 ± 0.1
Middle	5.0 ± 0.7	4.0 ± 0.3
Lower	5.0 ± 0.3	3.9 ± 0.4

The highest concentration of fluorine indicating NaCMC is in the middle for a lower drying rate. The upper and lower thirds show smaller amounts of fluorine. In comparison, the higher drying rate shows the highest amount of fluorine in the upper third, showing an increase of fluorine of 50% with regard to the slower drying rate. The middle and lower thirds both show a decline in concentration of fluorine, indicating a change in binder distribution. This is in line with current research, which suggests that NaCMC is migrating to the top and thereby negatively influences the battery performance.[19,22]

CONCLUSION

In this work, we showed a new staining method using (heptadecafluorodecyl)trimethoxysilane (HDF-TMS) to make NaCMC properly traceable by staining, without affecting the binder distribution. This is due to the HDF-TMS being applied in ethanol, not dissolving any binder and therefore hindering any redeposition. Additionally, no other electrode components show any side reactions, nor are there any significant traces of fluorine in the electrode when only submerging the electrode in the staining agent. This method allows us to compare different process parameters by simply using EDS on electrode cross sections, which was proven by staining the NaCMC in two electrodes with varying drying conditions. It was demonstrated for the first time that binder distribution of NaCMC is influenced by different drying conditions via visualization in EDS through staining.

ASSOCIATED CONTENT

Supporting Information

The Supporting Information is available free of charge at https://pubs.acs.org/doi/10.1021/acsaem.5c00048.

Detailed energy dispersive spectroscopy (EDS) results for all analyzed samples, with additional EDS mappings to complement the data presented in the main article (PDF)

AUTHOR INFORMATION

Corresponding Author

Noah Keim − *Institute for Applied Materials (IAM), Karlsruhe Institute of Technology (KIT), 76131 Karlsruhe, Germany*; orcid.org/0000-0002-3338-5811; Phone: +49 (0)721 608-22310; Email: noah.keim@kit.edu

Authors

Andreas Weber − *Institute for Applied Materials (IAM), Karlsruhe Institute of Technology (KIT), 76131 Karlsruhe, Germany*

Marcus Müller − *Institute for Applied Materials (IAM), Karlsruhe Institute of Technology (KIT), 76131 Karlsruhe, Germany*; orcid.org/0000-0002-5562-7201

David Burger − *Thin Film Technology (TFT), Karlsruhe Institute of Technology (KIT), 76131 Karlsruhe, Germany*

Werner Bauer − *Institute for Applied Materials (IAM), Karlsruhe Institute of Technology (KIT), 76131 Karlsruhe, Germany*; orcid.org/0000-0002-5923-2426

Philip Scharfer − *Thin Film Technology (TFT), Karlsruhe Institute of Technology (KIT), 76131 Karlsruhe, Germany*

Wilhelm Schabel − *Thin Film Technology (TFT), Karlsruhe Institute of Technology (KIT), 76131 Karlsruhe, Germany*

Helmut Ehrenberg − *Institute for Applied Materials (IAM), Karlsruhe Institute of Technology (KIT), 76131 Karlsruhe, Germany*; orcid.org/0000-0002-5134-7130

Complete contact information is available at: https://pubs.acs.org/10.1021/acsaem.5c00048

Notes

The authors declare no competing financial interest.

■ ACKNOWLEDGMENTS

This work contributes to the research performed at CELEST (Center for Electrochemical Energy Storage Ulm Karlsruhe) and Material Research Center for Energy Systems (MZE). The authors thank Roland Bayer and Oliver Petermann (IFF N&H Germany GmbH & Co. KG) for providing the binders and fruitful discussions.

■ REFERENCES

(1) Chen, J.-M.; Hsu, C.-H.; Lin, Y.-R.; Hsiao, M.-H.; Fey, G. T.-K. High-power LiFePO4 cathode materials with a continuous nano carbon network for lithium-ion batteries. *J. Power Sources* **2008**, *184*, 498−502.

(2) Kraytsberg, A.; Ein-Eli, Y. Higher, Stronger, Better: A Review of 5 V Cathode Materials for Advanced Lithium-Ion Batteries. *Adv. Energy Mater.* **2012**, *2*, 922−939.

(3) Lingappan, N.; Kong, L.; Pecht, M. The significance of aqueous binders in lithium-ion batteries. *Renew. Sustain. Energy Rev.* **2021**, *147*, 111227.

(4) Liu, S.; Xiong, L.; He, C. Long cycle life lithium ion battery with lithium nickel cobalt manganese oxide (NCM) cathode. *J. Power Sources* **2014**, *261*, 285−291.

(5) Li, J.; Fleetwood, J.; Hawley, W. B.; Kays, W. From Materials to Cell: State-of-the-Art and Prospective Technologies for Lithium-Ion Battery Electrode Processing. *Chem. Rev.* **2022**, *122*, 903−956.

(6) Stahl, T.; Mattern, D.; Brunn, H. Toxicology of perfluorinated compounds. *Environ. Sci. Eur.* **2011**, *23*, 38.

(7) Sitarek, K.; Stetkiewicz, J.; Wasowicz, W. Evaluation of Reproductive Disorders in Female Rats Exposed to -Methyl-2-Pyrrolidone. *Birth Defects Res. B Dev. Reprod. Toxicol.* **2012**, *95*, 195−201.

(8) Sitarek, K.; Stetkiewicz, J. Assessment of reproductive toxicity and gonadotoxic potential of N-methyl-2-pyrrolidone in male rats. *Int. J. Occup. Med. Environ. Health* **2008**, *21*, 73−80.

(9) Müller, M.; Pfaffmann, L.; Jaiser, S.; Baunach, M.; Trouillet, V.; Scheiba, F.; Scharfer, P.; Schabel, W.; Bauer, W. Investigation of binder distribution in graphite anodes for lithium-ion batteries. *J. Power Sources* **2017**, *340*, 1−5.

(10) Jaiser, S.; Müller, M.; Baunach, M.; Bauer, W.; Scharfer, P.; Schabel, W. Investigation of film solidification and binder migration during drying of Li-Ion battery anodes. *J. Power Sources* **2016**, *318*, 210−219.

(11) Buqa, H.; Holzapfel, M.; Krumeich, F.; Veit, C.; Novák, P. Study of styrene butadiene rubber and sodium methyl cellulose as binder for negative electrodes in lithium-ion batteries. *J. Power Sources* **2006**, *161*, 617−622.

(12) Lee, J.-H.; Lee, S.; Paik, U.; Choi, Y.-M. Aqueous processing of natural graphite particulates for lithium-ion battery anodes and their electrochemical performance. *J. Power Sources* **2005**, *147*, 249−255.

(13) Bresser, D.; Buchholz, D.; Moretti, A.; Varzi, A.; Passerini, S. Alternative binders for sustainable electrochemical energy storage − the transition to aqueous electrode processing and bio-derived polymers. *Energy Environ. Sci.* **2018**, *11*, 3096−3127.

(14) Courtel, F. M.; Niketic, S.; Duguay, D.; Abu-Lebdeh, Y.; Davidson, I. J. Water-soluble binders for MCMB carbon anodes for lithium-ion batteries. *J. Power Sources* **2011**, *196*, 2128−2134.

(15) Qiu, L.; Shao, Z.; Wang, D.; Wang, F.; Wang, W.; Wang, J. Carboxymethyl cellulose lithium (CMC-Li) as a novel binder and its electrochemical performance in lithium-ion batteries. *Cellulose* **2014**, *21*, 2789−2796.

(16) Keim, N.; Weber, A.; Müller, M.; Kaufmann, U.; Bauer, W.; Petermann, O.; Bayer, R.; Ehrenberg, H. Understanding Key NaCMC Properties to Optimize Electrodes and Battery Performance. *Adv. Energy Sustainability Res.* **2025**, *6*, 2400364.

(17) Lee, J.-H.; Kim, J.; Jeong, M. H.; Ahn, K. H.; Lee, H. L.; Youn, H. J. Visualization of styrene-butadiene rubber (SBR) latex and large-scale analysis of the microstructure of lithium-ion battery (LIB) anodes. *J. Power Sources* **2023**, *557*, 232552.

(18) Burger, D.; Klemens, J.; Keim, N.; Müller, M.; Bauer, W.; Schmatz, J.; Kumberg, J.; Scharfer, P.; Schabel, W. Additive Influence on Binder Migration in Electrode Drying. *Energy Technol.* **2024**, *12*, 2400057.

(19) Park, K.; Ryu, M.; Jung, Y.; Yoo, H. E.; Myeong, S.; Lee, D.; Kim, S. C.; Kim, C.; Kim, J.; Kwon, J.; Lee, K.; Cho, C.-W.; Paik, U.; Song, T. Mitigation of Binder Migration Behavior during the Drying Process by Applying an Electric Field for Fast-Charging in Lithium-Ion Batteries. *Batter. Supercaps* **2023**, *6*, No. e202300170.

(20) Gadhave, R. V.; Dhawale, P. V.; Sorate, C. S. Surface modification of cellulose with silanes for adhesive application. *Open J. Polym. Chem.* **2021**, *11*, 11−30.

(21) Yuan, Y.; Lin, H.; Yu, D.; Yin, Y.; Tang, B.; Li, E.; Zhang, S. Effects of perfluorooctyltriethoxysilane coupling agent on the properties of silica filled PTFE composites. *J. Mater. Sci.: Mater. Electron.* **2017**, *28*, 8810−8817.

(22) Burger, D.; Keim, N.; Shabbir, J.; Gao, Y.; Müller, M.; Bauer, W.; Hoffmann, A.; Scharfer, P.; Schabel, W. Simultaneous Primer Coating for Fast Drying of Battery Electrodes. *Energy Technol.* **2025**, *13*, 2401668.

https://doi.org/10.1021/acsaem.5c00048
ACS Appl. Energy Mater. XXXX, XXX, XXX−XXX